Supporting Information

Contribution from College of Materials Science and Opto-electronic Technology,

University of Chinese Academy of Sciences,

19A Yuquan Road, Beijing, China 100049 and

Department of Chemistry and Biochemistry,

University of Notre Dame, Notre Dame, Indiana 46556 and

Department of Physics, Knox College, Galesburg, Illinois 61401, USA

Correlated Ligand Dynamics in Oxyiron Picket Fence Porphyrins: Structural and Mössbauer Investigations

Jianfeng Li,[†,‡,*] Bruce C. Noll,[‡] Allen G. Oliver,[‡] Charles E. Schulz,[§] and W. Robert Scheidt[‡,*]

[†]University of Chinese Academy of Sciences

[‡]University of Notre Dame

[§]Knox College

[*]To whom correspondence should be addressed. E-mail: JL: jfli@ucas.ac.cn, CES: cshulz@knox.edu, WRS: scheidt.1@nd.edu

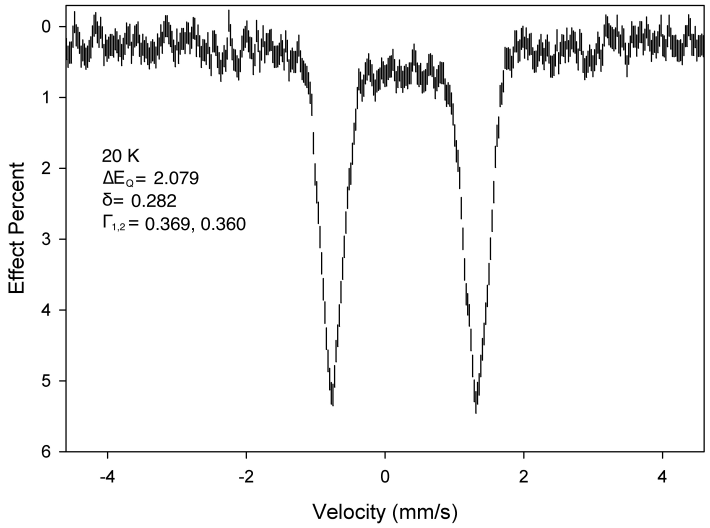
20 K
ΔE_Q= 2.079
δ= 0.282
Γ_1,2= 0.369, 0.360
Effect Percent
Velocity (mm/s)

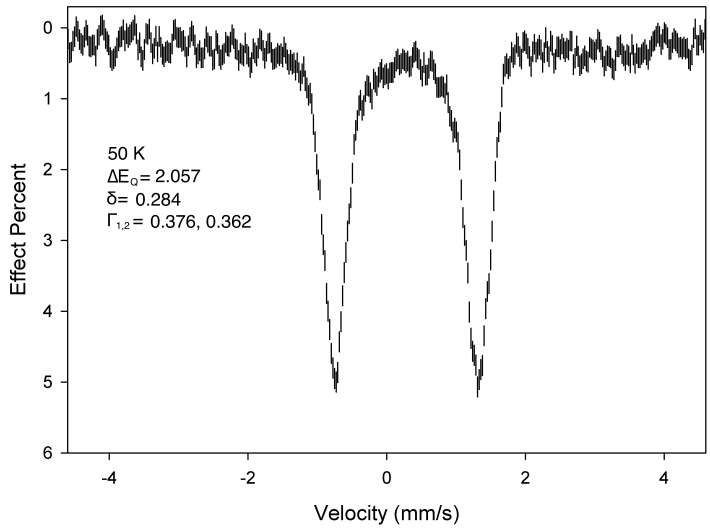
50 K
ΔE_Q= 2.057
δ= 0.284
Γ_1,2= 0.376, 0.362
Effect Percent
Velocity (mm/s)

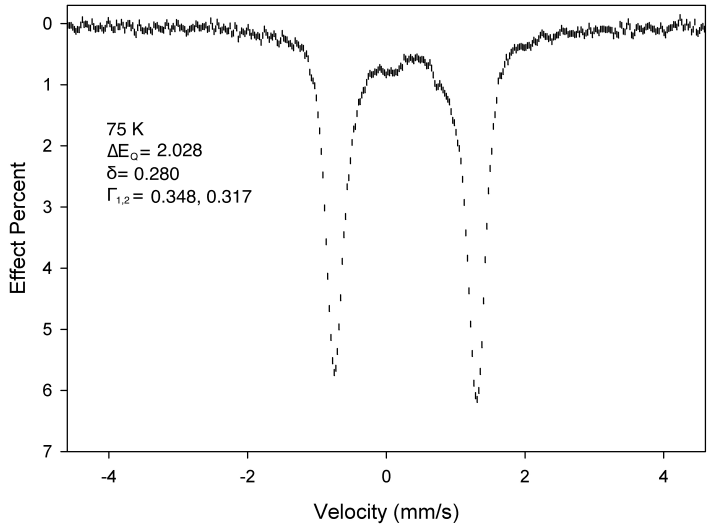
75 K
ΔE_Q= 2.028
δ= 0.280
Γ_1,2= 0.348, 0.317
Effect Percent
Velocity (mm/s)

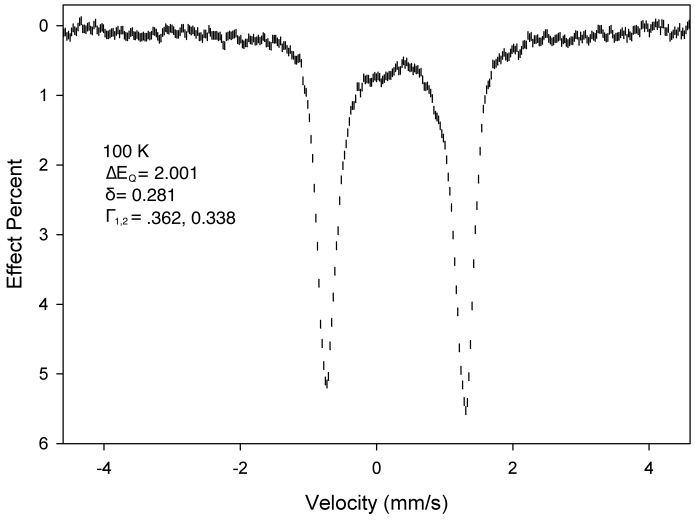
100 K
ΔE_Q= 2.001
δ= 0.281
Γ_1,2= .362, 0.338
Effect Percent
Velocity (mm/s)

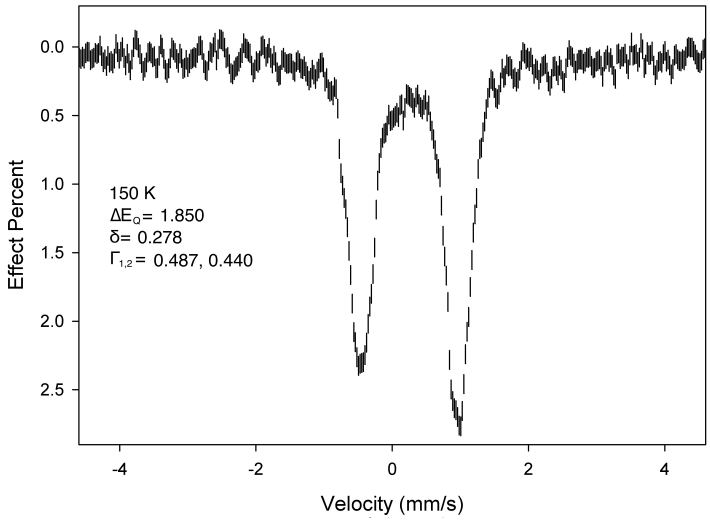
150 K
ΔE_Q= 1.850
δ= 0.278
Γ_1,2= 0.487, 0.440
Effect Percent
Velocity (mm/s)

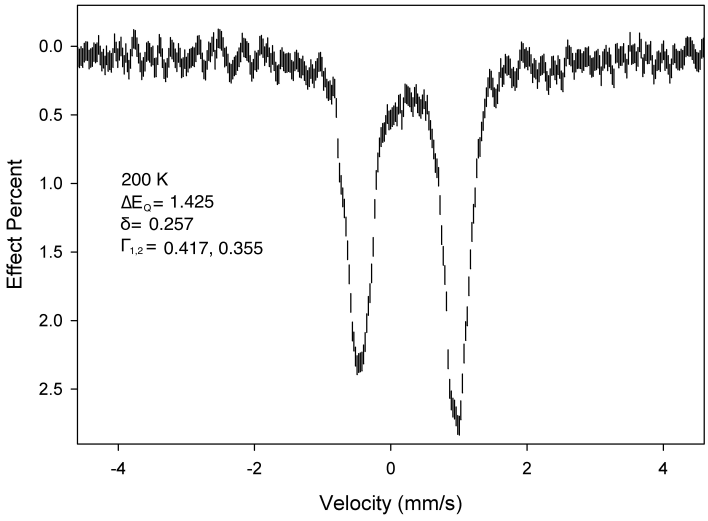
200 K
ΔE_Q= 1.425
δ= 0.257
Γ_1,2= 0.417, 0.355
Effect Percent
Velocity (mm/s)

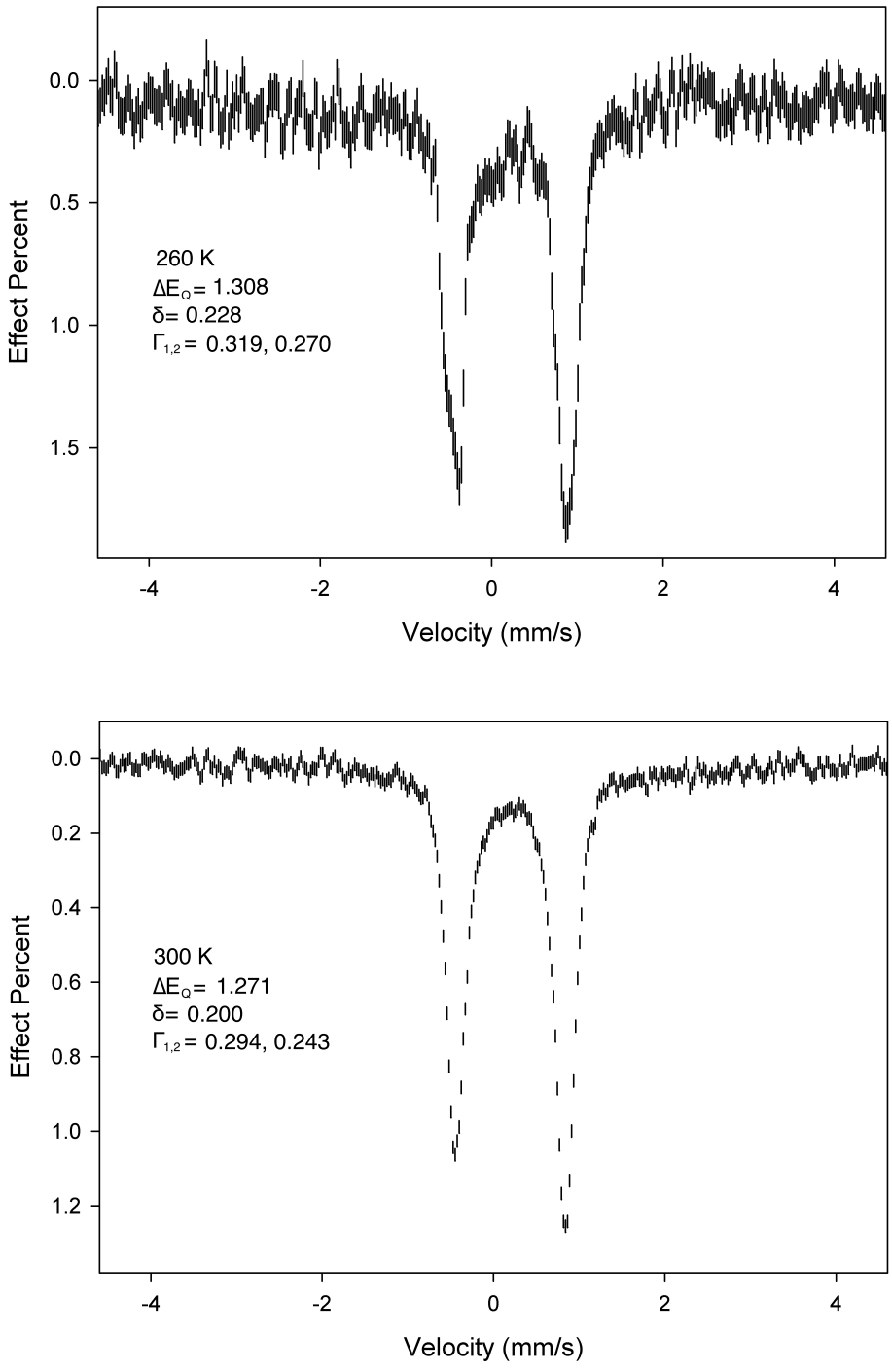

Figure S1. Figures showing experimental Mössbauer spectra for [Fe(TpivPP)(1-EtIm)(O_2)] over a range of temperatures.

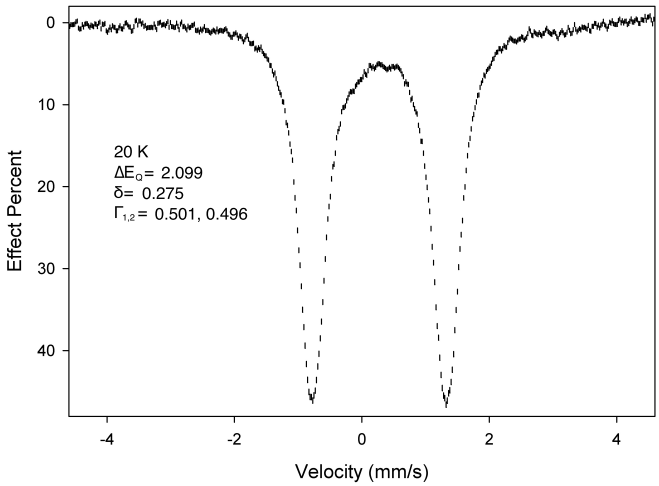
20 K
ΔE_Q = 2.099
δ = 0.275
Γ_1,2 = 0.501, 0.496
Effect Percent
Velocity (mm/s)

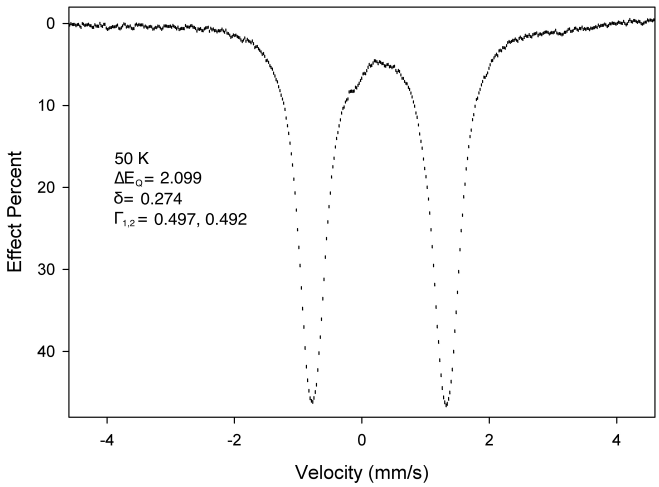
50 K
ΔE_Q = 2.099
δ = 0.274
Γ_1,2 = 0.497, 0.492
Effect Percent
Velocity (mm/s)

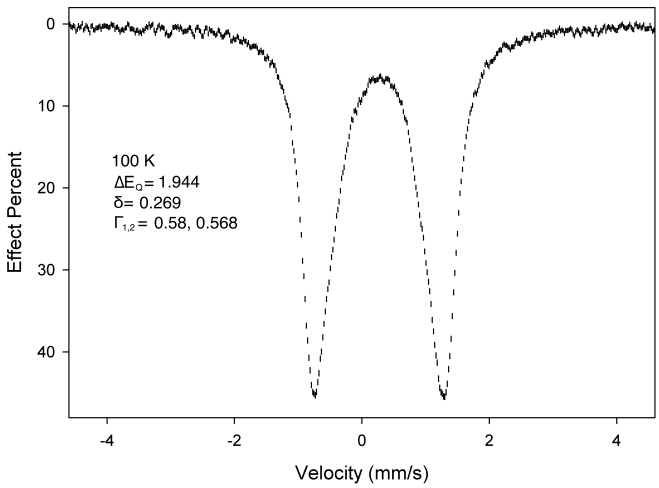
100 K
ΔE_Q = 1.944
δ = 0.269
Γ_1,2 = 0.58, 0.568
Effect Percent
Velocity (mm/s)

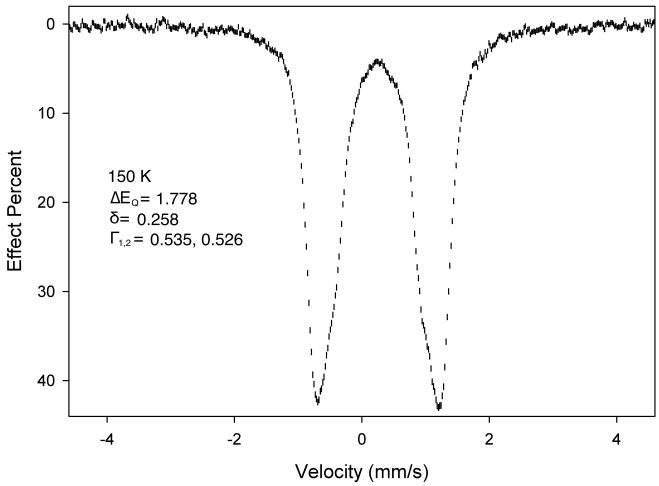
150 K
ΔE_Q = 1.778
δ = 0.258
Γ_1,2 = 0.535, 0.526
Effect Percent
Velocity (mm/s)

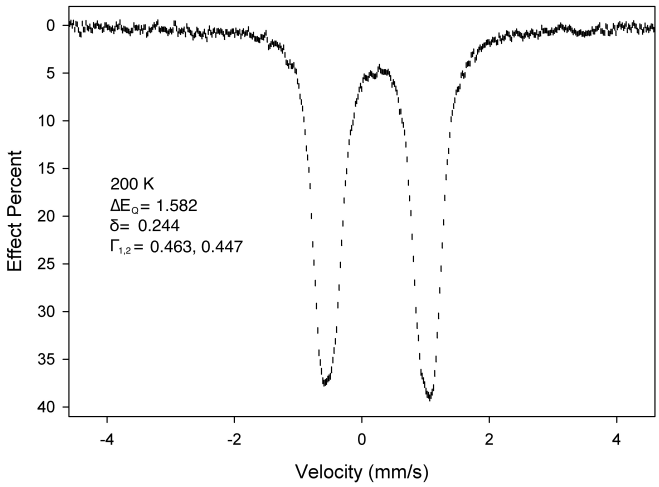
200 K
ΔE_Q = 1.582
δ = 0.244
Γ_1,2 = 0.463, 0.447
Effect Percent
Velocity (mm/s)

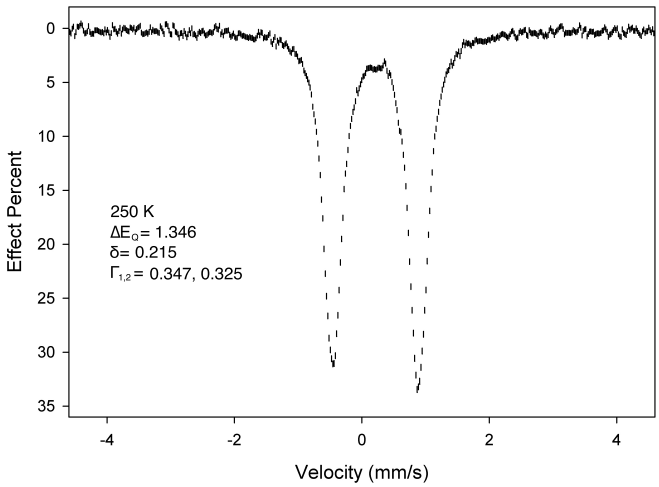
250 K
ΔE_Q = 1.346
δ = 0.215
Γ_1,2 = 0.347, 0.325
Effect Percent
Velocity (mm/s)

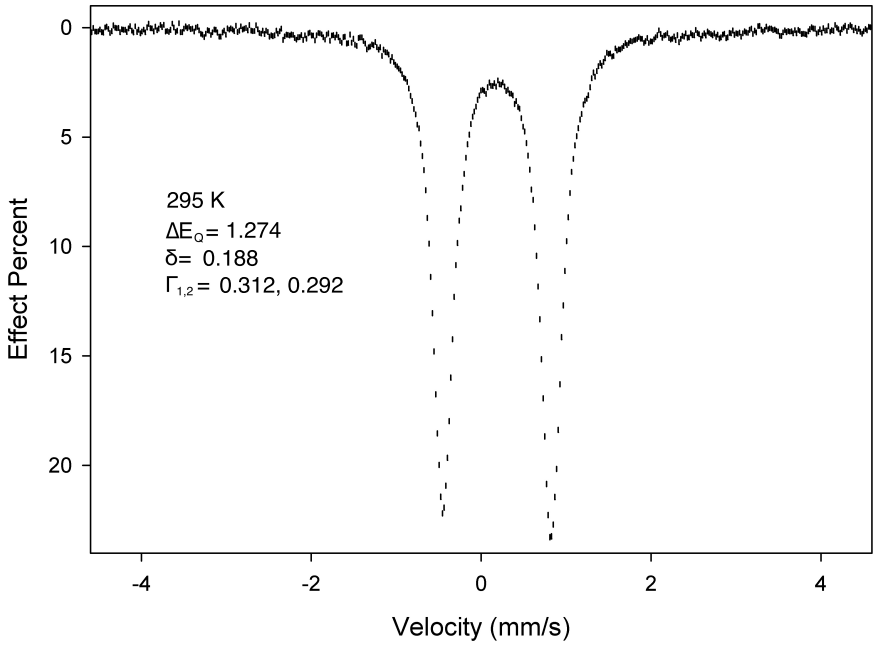

Figure S2. Figures showing experimental Mössbauer spectra for [Fe(TpivPP)(1-MeIm)(O_2)] over a range of temperatures.

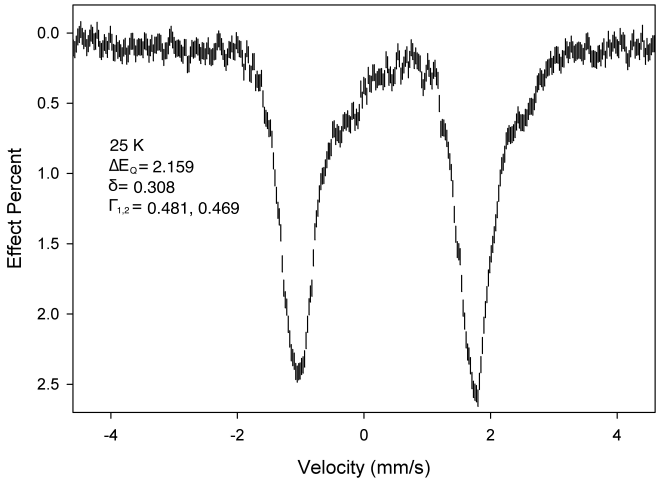
25 K
ΔE_Q= 2.159
δ= 0.308
Γ_1,2= 0.481, 0.469
Effect Percent
Velocity (mm/s)

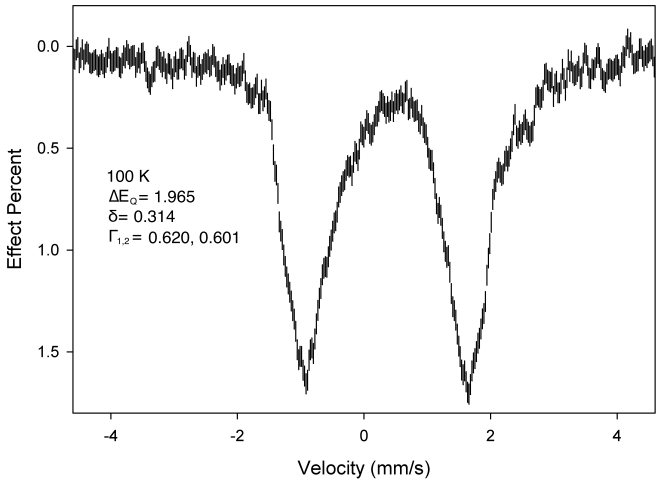
100 K
ΔE_Q= 1.965
δ= 0.314
Γ_1,2= 0.620, 0.601
Effect Percent
Velocity (mm/s)

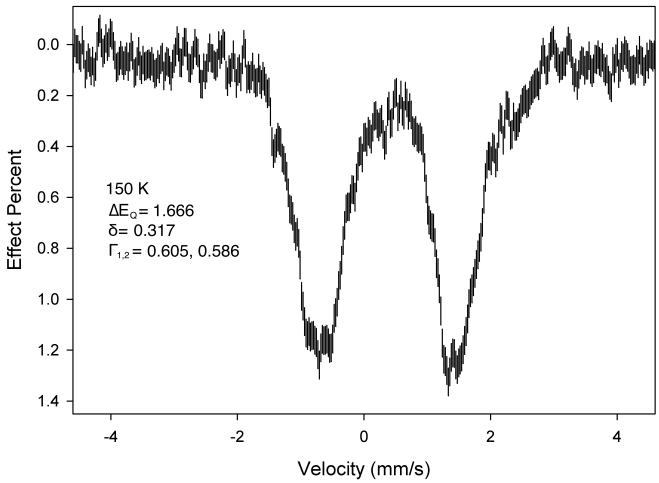
150 K
ΔE_Q= 1.666
δ= 0.317
Γ_1,2= 0.605, 0.586
Effect Percent
Velocity (mm/s)

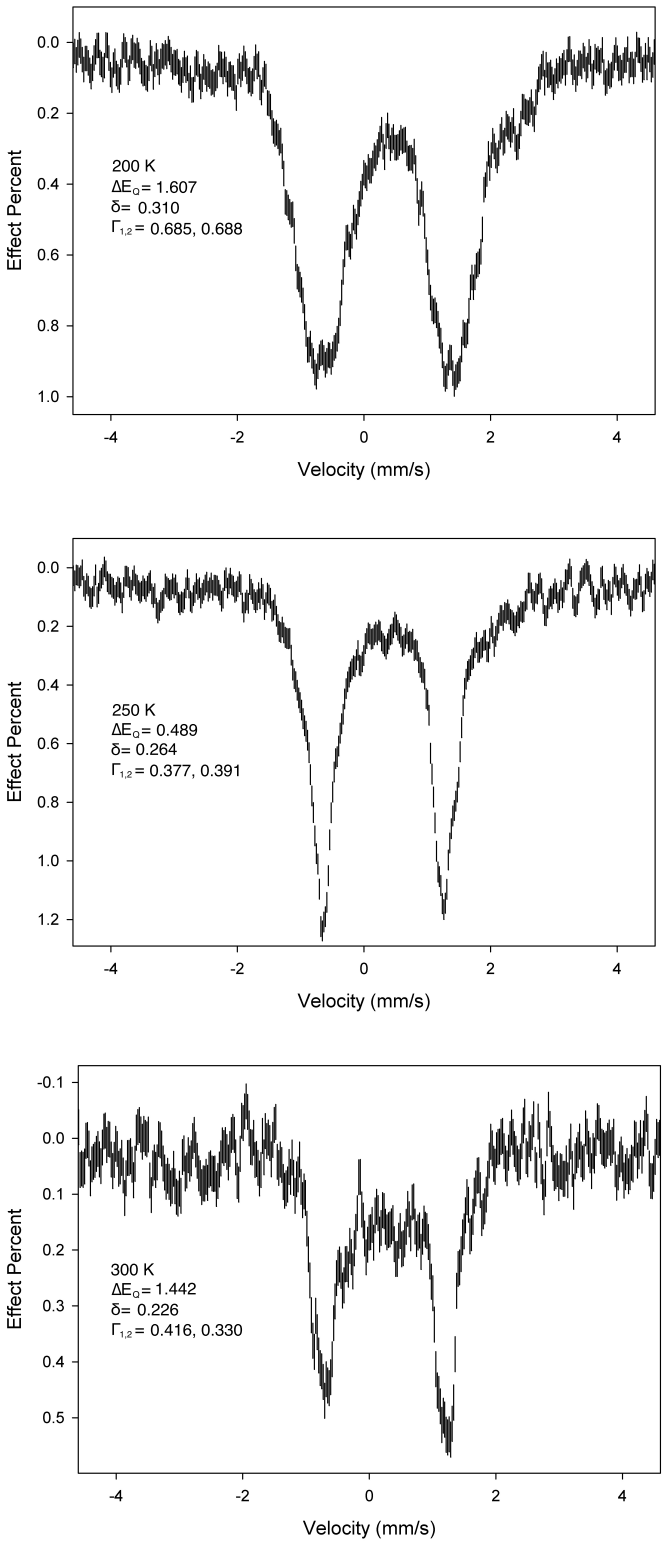

Figure S3. Figures showing experimental Mössbauer spectra for [Fe(TpivPP)(2-MeHIm)(O_2)] over a range of temperatures.

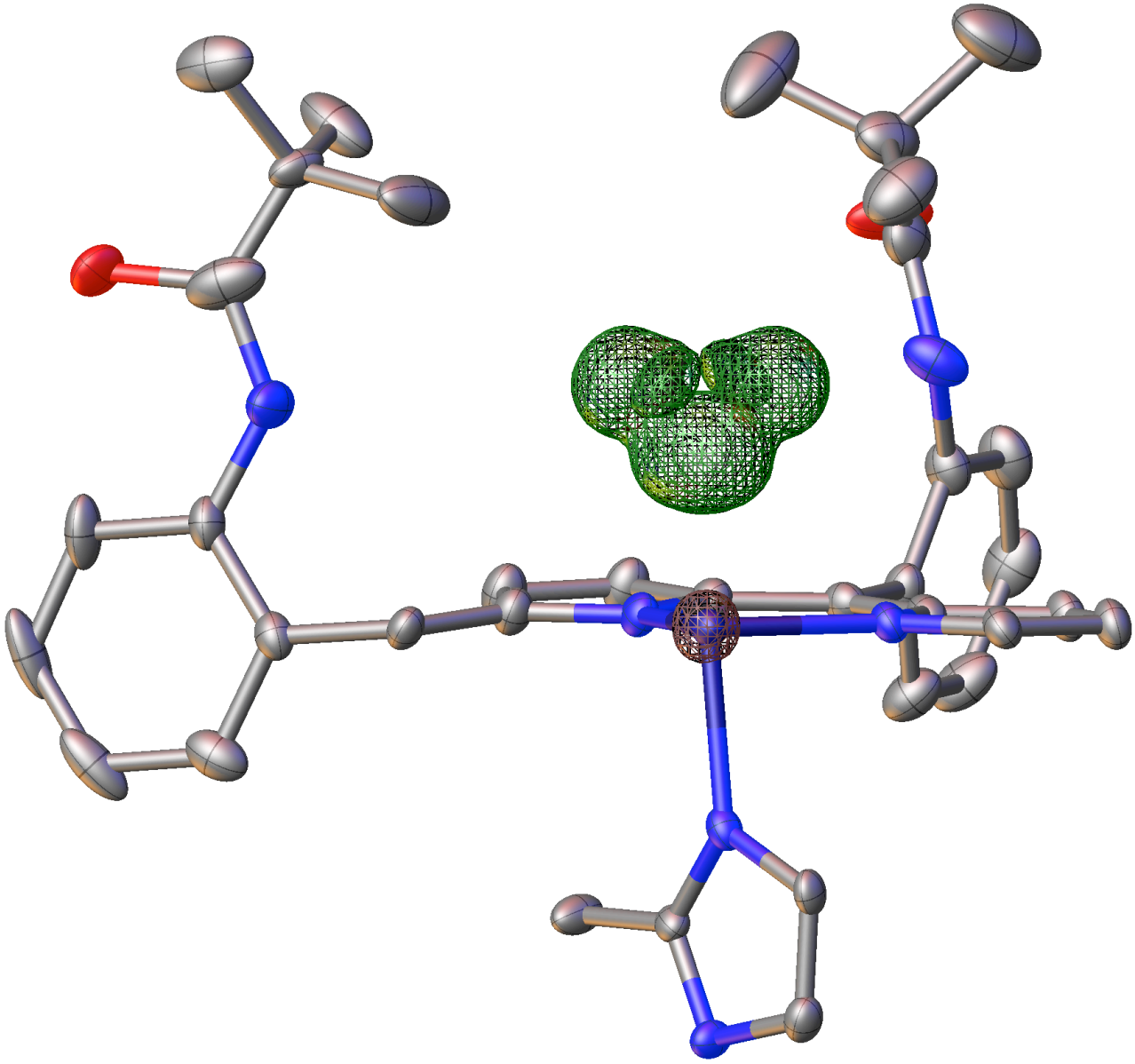

Figure S4. Difference electron density at the oxygen site at 80K. Only the asymmetric unit of structure is displayed. The major and minor terminal oxygen atoms are clearly visible.

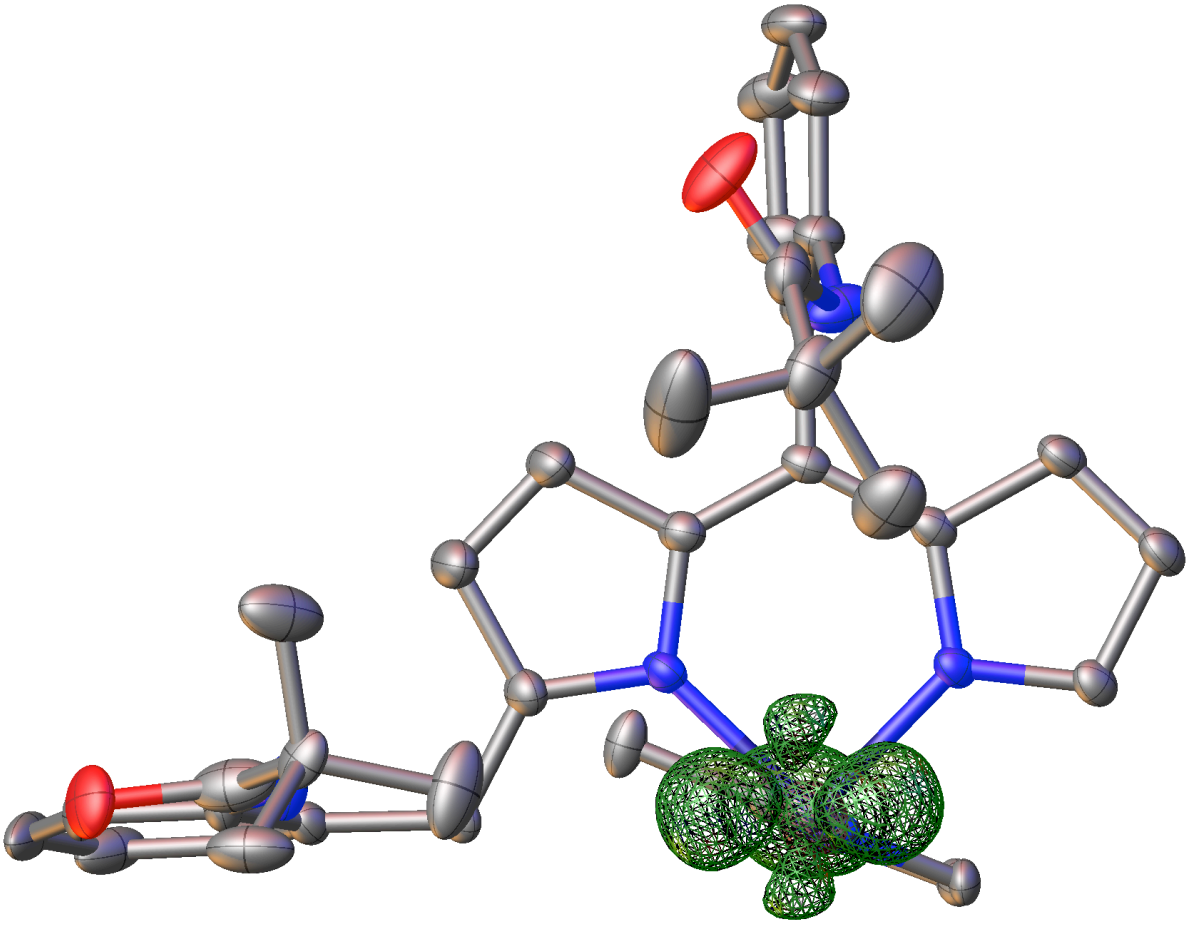

Figure S5. Difference electron density at the oxygen site at 80K. Only the asymmetric unit of structure is displayed. The major and minor terminal oxygen atoms are clearly visible. Note that in this illustration the unfavorable orientation of the methyl group of the picket is illustrated (left).

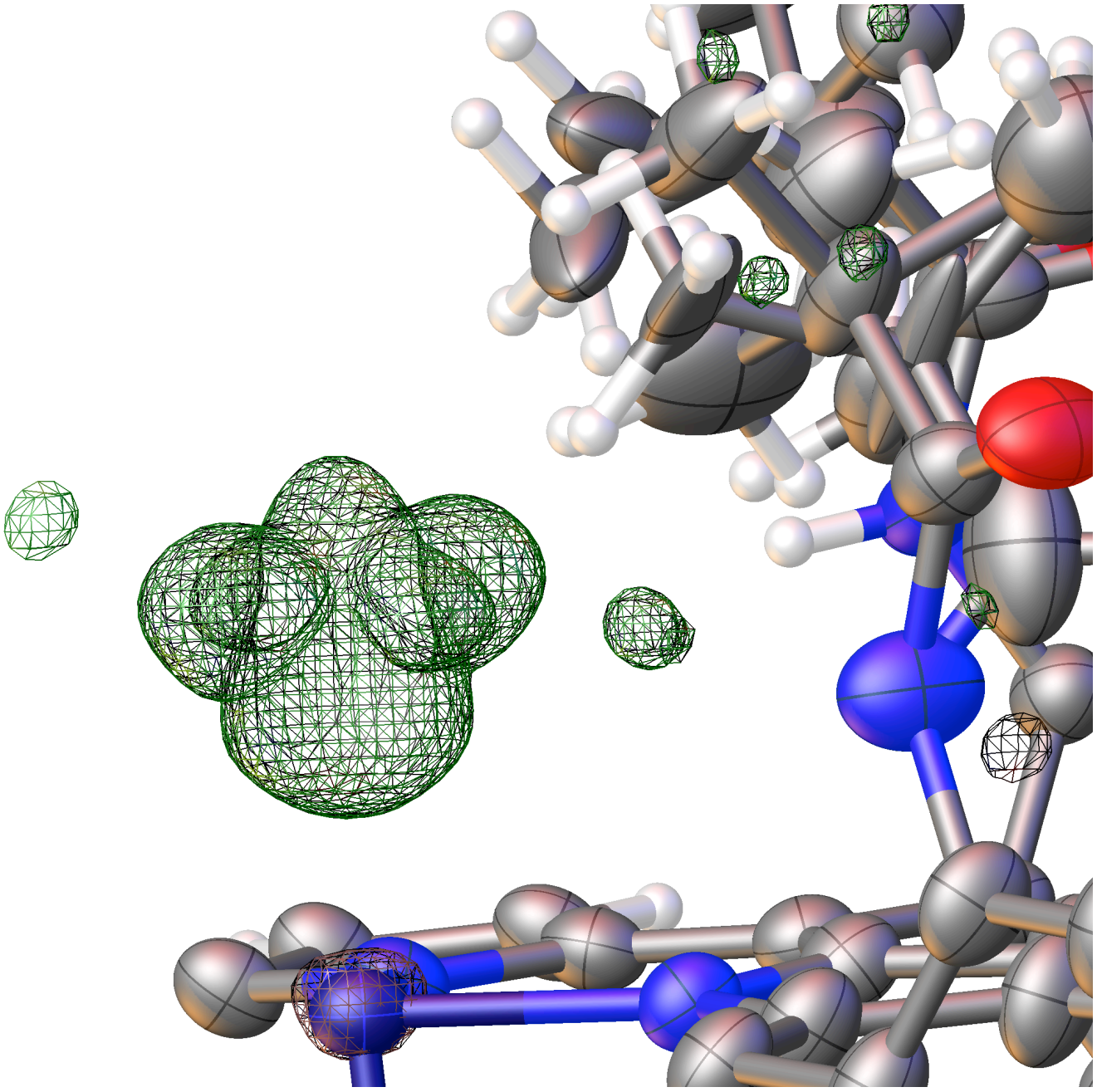

Figure S6. Electron density at the oxygen site of [Fe(TpivPP)(1-MeIm)(O_2)] at 100K. Only the asymmetric unit of structure is displayed. .

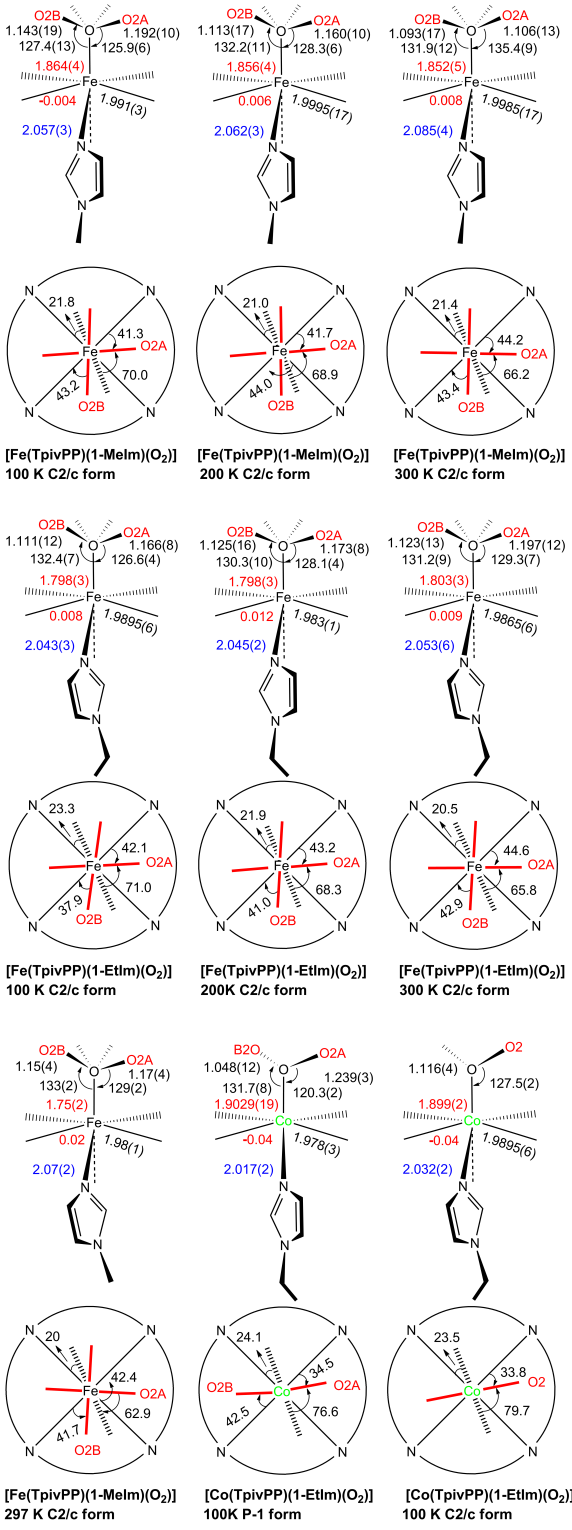

Figure S7. Formal diagrams of structures of [Fe(TpivPP)(1-MeIm)(O_2)][?b] and [Co(TpivPP)(1-EtIm)(O_2)] at different temperatures and space groups. The upper schemes are edge-on view of the porphyrin plane and ligands with the key parameters (distances in Å, angle in degrees) shown in sequence of O–O, O–O–M, M–O, Δ_{24} (positive to proximal side), M–N_p and M–N_{ax}. The below schemes are top view of the porphyrin plane showing the projections of dioxygen (red line) and imidazole plane (dash line) and their angles between the closet M–N_p vectors.

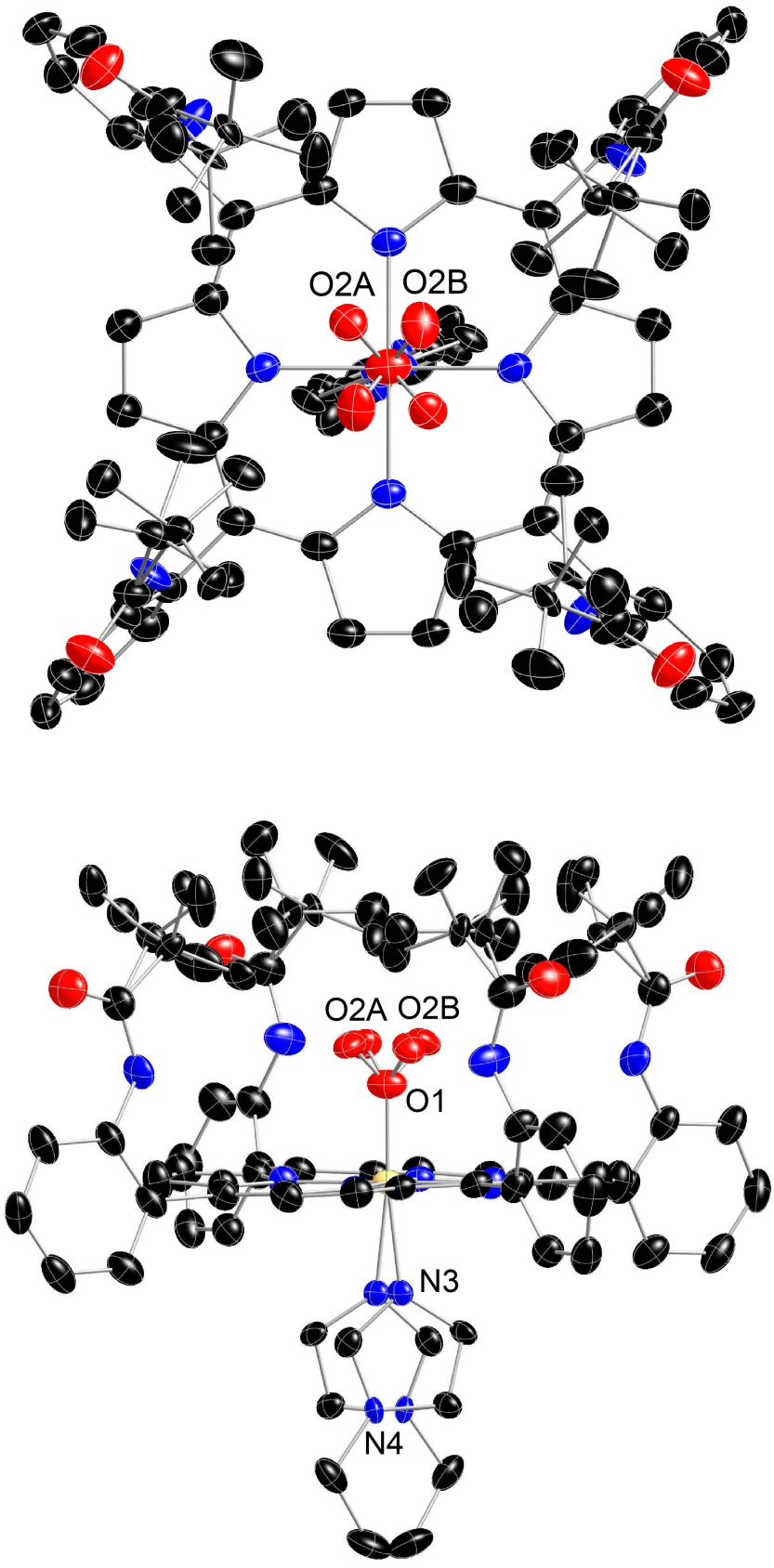

Figure S8. Top and side thermal ellipsoid views of [Fe(TpivPP)(1-EtIm)(O_2)] at 100K. 50% probability ellipsoids are shown.

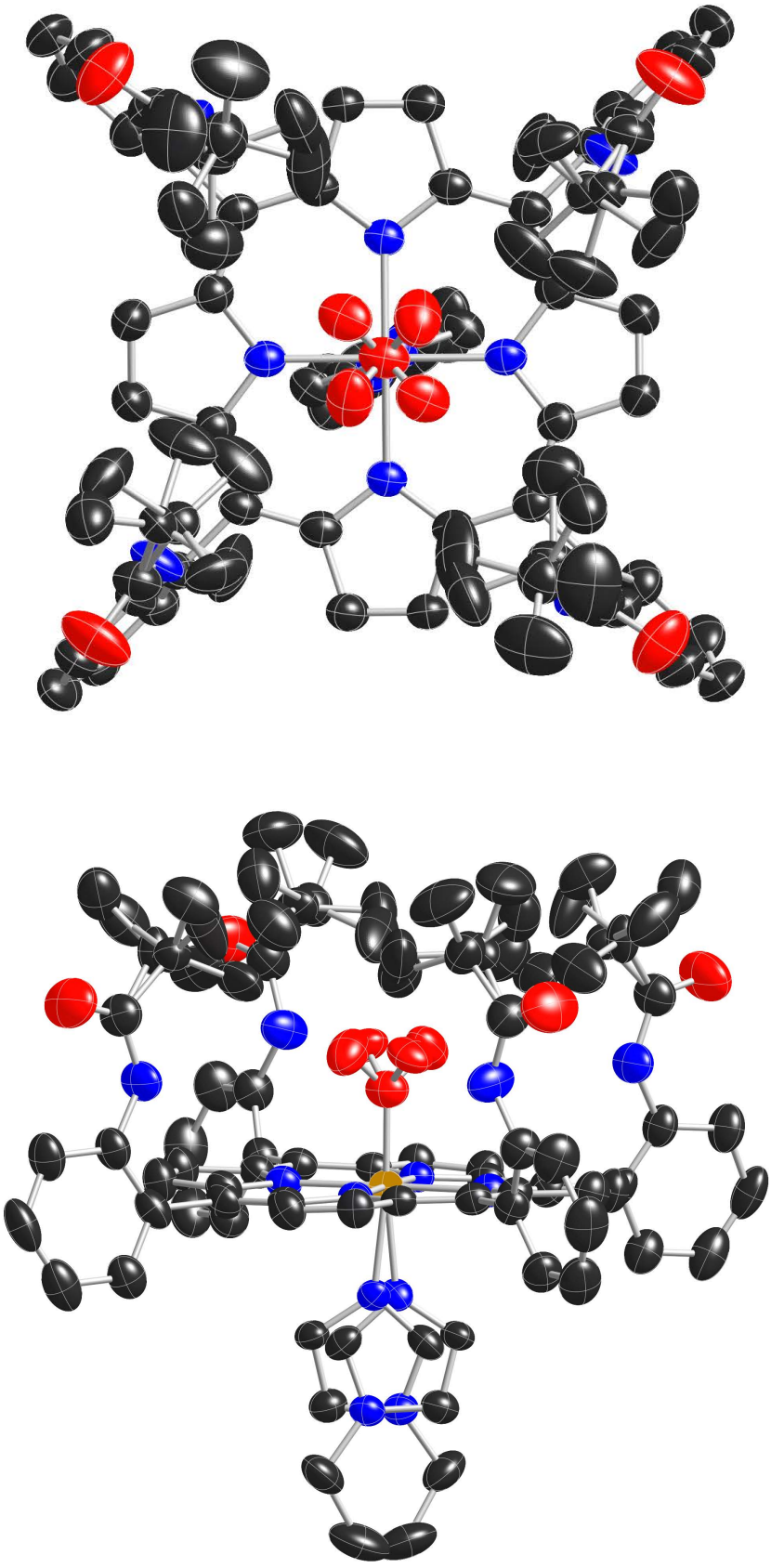

Figure S9. Top and side thermal ellipsoid views of [Fe(TpivPP)(1-EtIm)(O_2)] at 200K. 50% probability ellipsoids are shown.

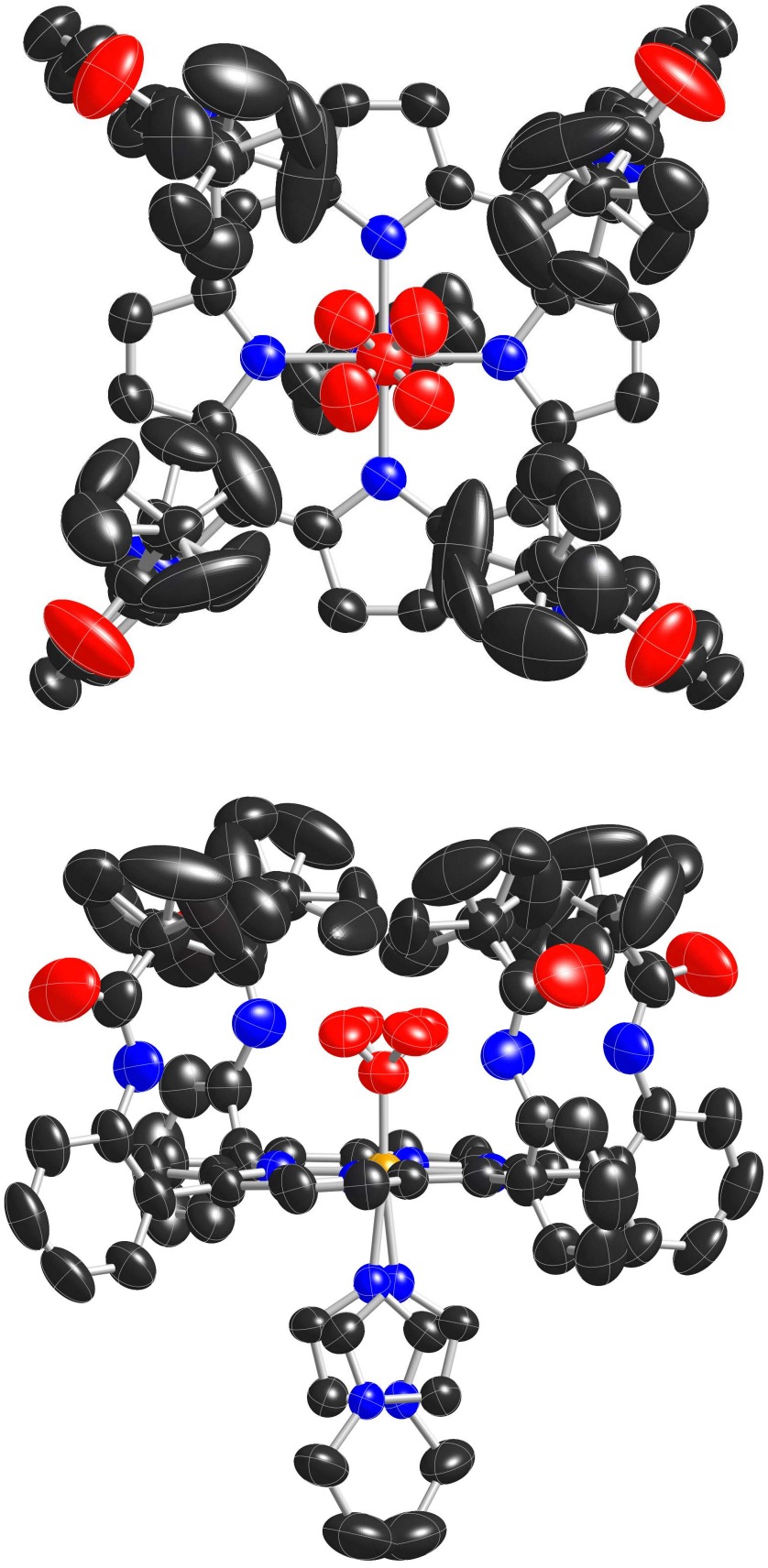

Figure S10. Top and side thermal ellipsoid views of [Fe(TpivPP)(1-EtIm)(O_2)] at 300K. 50% probability ellipsoids are shown.

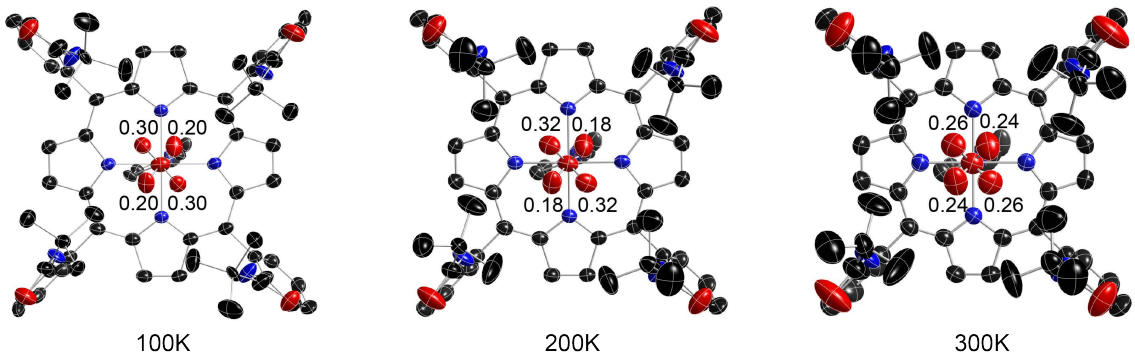

Figure S11. Thermal ellipsoid diagrams of [Fe(TpivPP)(1-EtIm)(O2)] structures at 100, 200 and 300 K (top view), with the terminal oxygen populations indicated. One of the two orientations are shown for axial imidazole and t-butyl groups which are disordered over two positions. Thermal ellipsoids are contoured at the 50% probability level for 100 K and 40% for 200 and 300 K. Hydrogen atoms omitted for clarity.

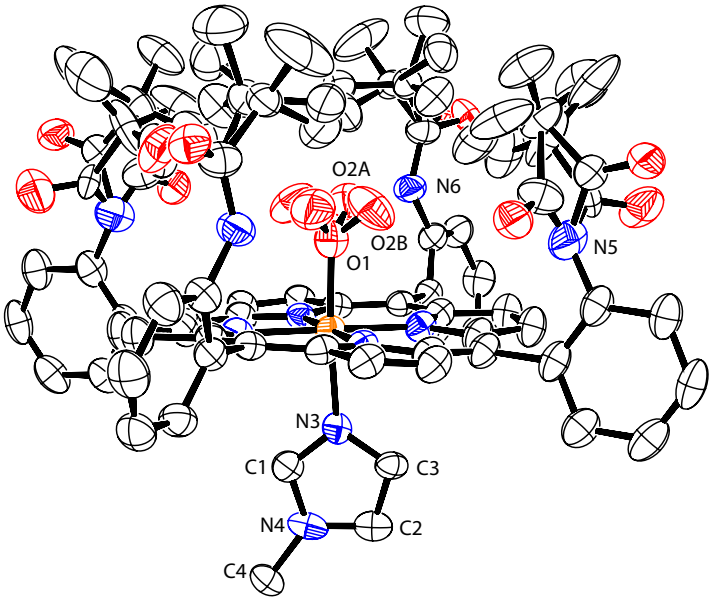

Figure S12. Figure showing an edge-on view of [Fe(TpivPP)(1-MeIm)(O_2)].

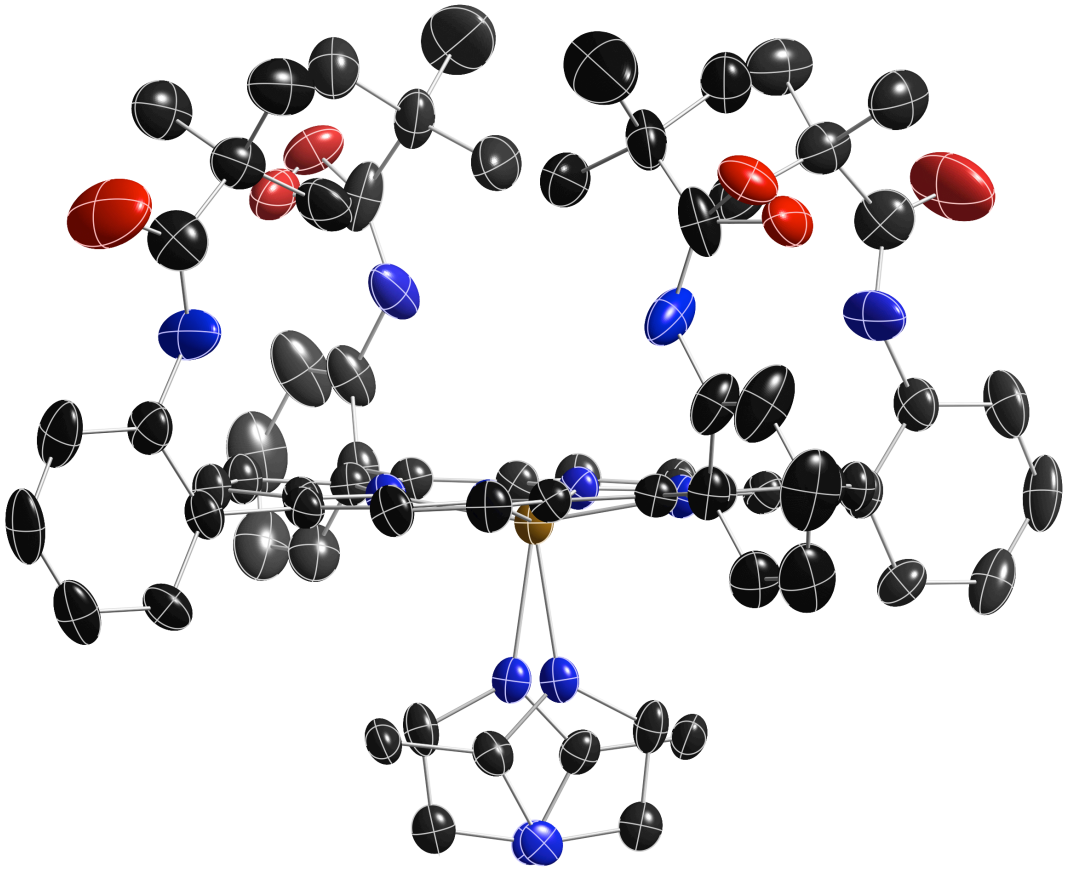

Figure S13. Thermal ellipsoid plot of [Fe(TpivPP)(2-MeHIm)] at 100 K, 50% probability ellipsoids are shown. The crystallographically required twofold axis is in the plane of the drawing and vertical.

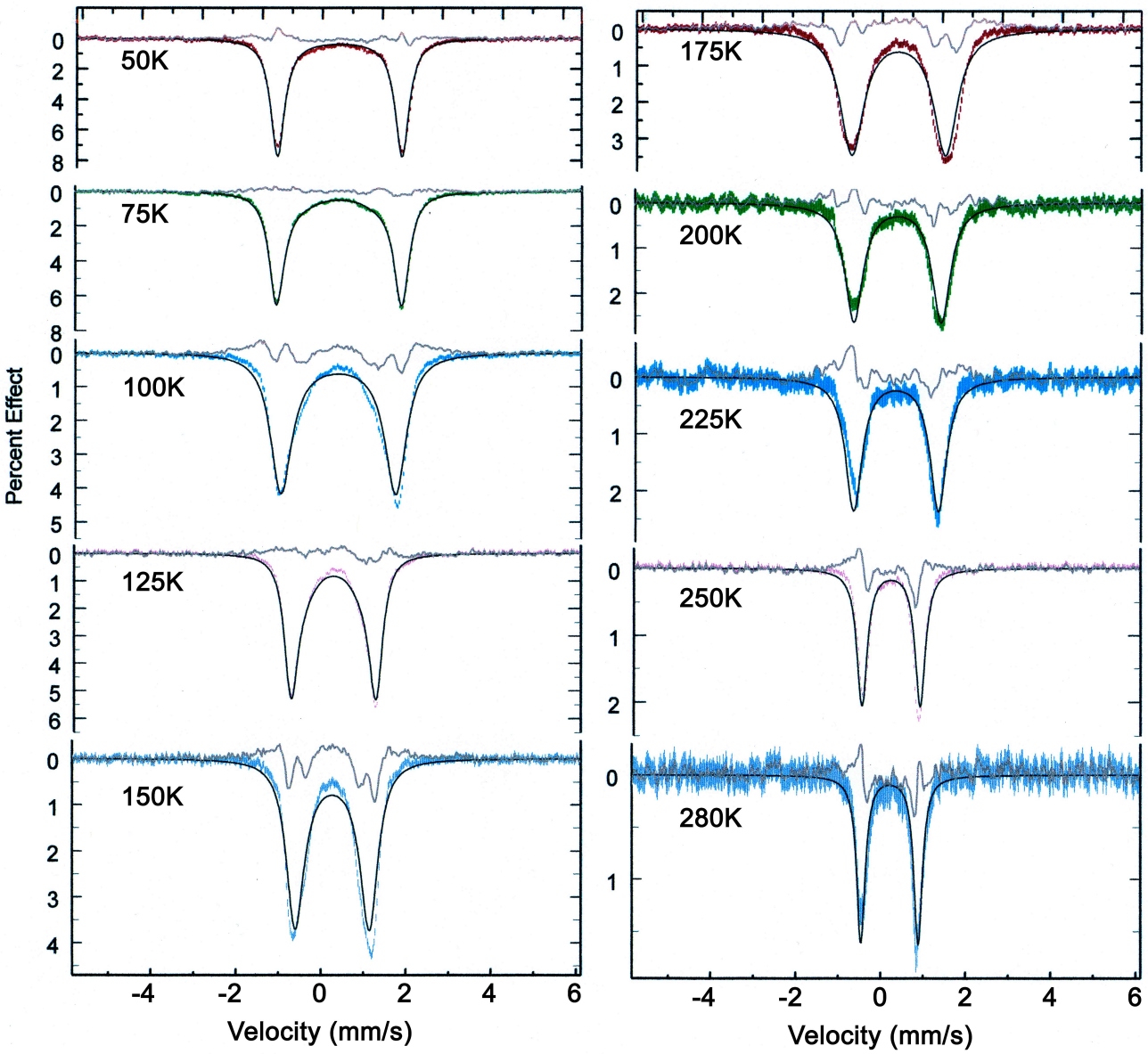

Figure S14. Comparison of the T-dependent experimental data for [Fe(TpivPP)(1-EtIm)(O_2)] with the predicted fits based on the model due to Lang et al. Parameters: QS(I)= −2.08 mm/s, η(I) = 0.19, QS(II)= −1.31 mm/s, η(II) = 0.90, energy difference = 103 cm^{-1}, line width = 0.23 mm/s, rate of interconversion = 1.24 × 10^6 sec^{-1} (50 K), 4.34 × 10^8 sec^{-1} (250 K), jump angle 90°. Fit residuals between the experimental data and the simulation are shown as the top line.

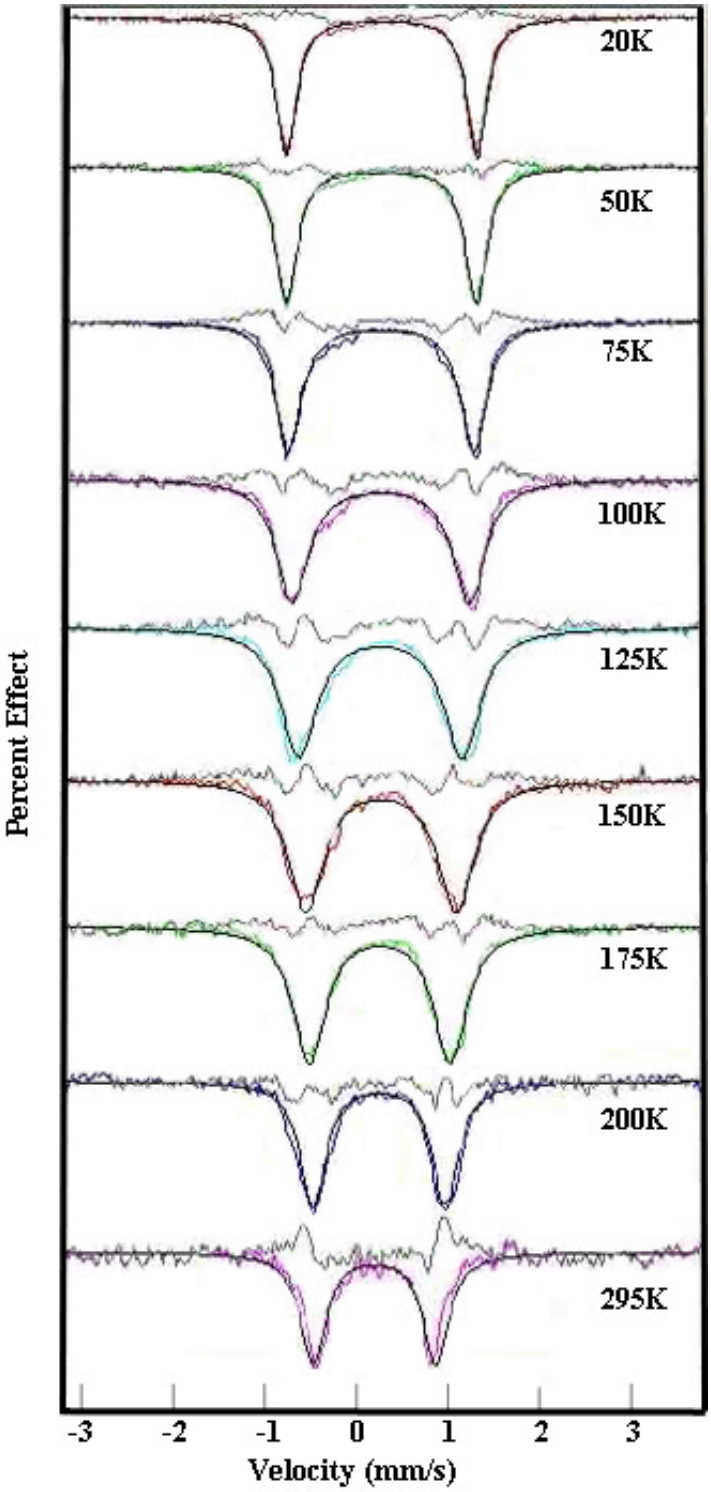

Figure S15. Simulation of the temperature dependent spectra for [Fe(TpivPP)(1-MeIm)(O_2)] based on the Oldfield model. Parameters: QS= -2.08 mm/s, $\eta = 0.18$, energy difference = 138 cm^{-1}, line width = 0.26 mm/s, rate of interconversion = 1.04×10^6 sec^{-1} (50 K), 3.25×10^8 sec^{-1} (200 K), jump angle 90°. Fit residuals between the experimental data and the simulation are shown as the top line.

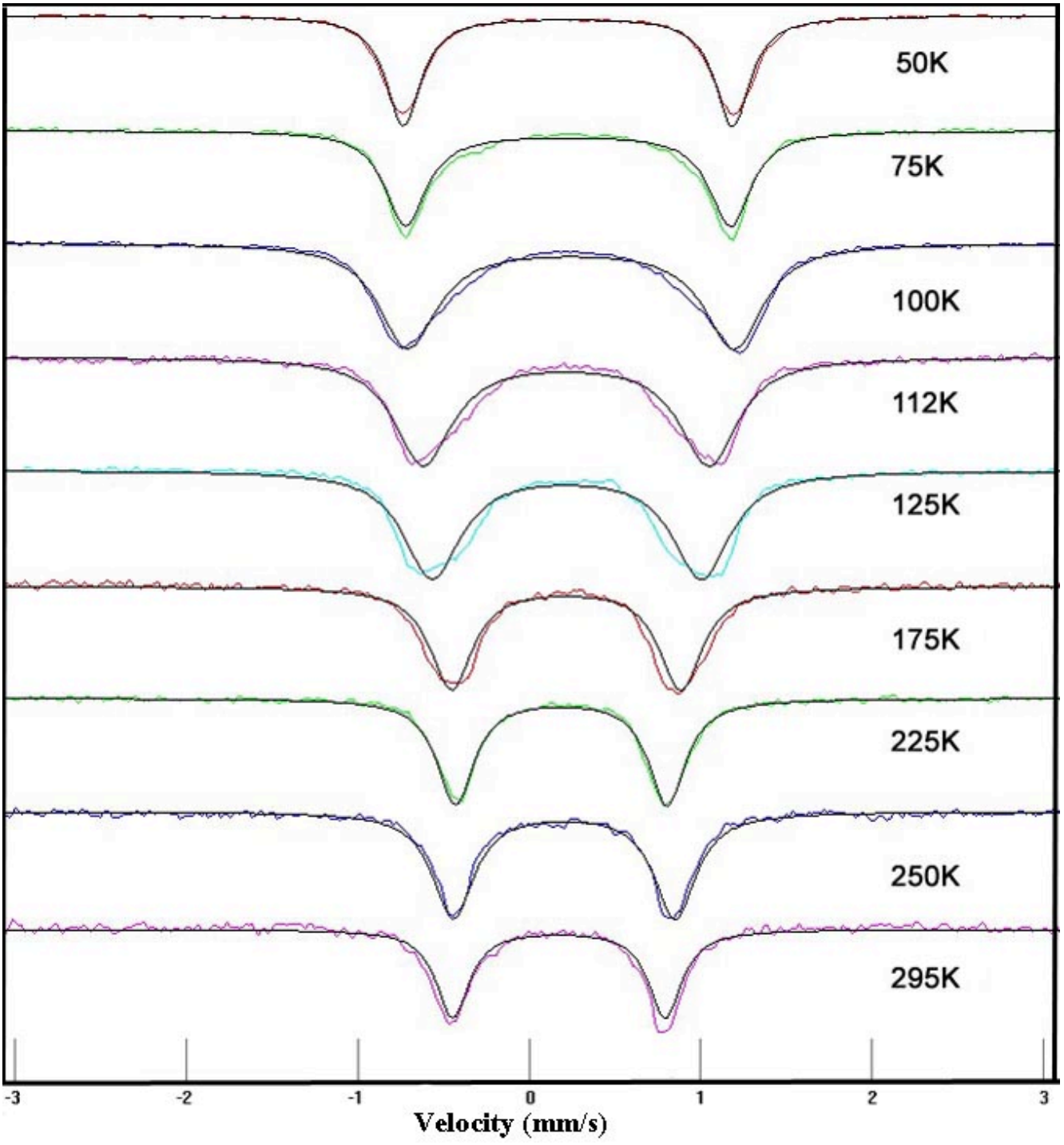

Figure S16. Comparison of the T-dependent experimental data for [Fe(TpivPP)(1-EtIm)(O_2)] (Sample 2) with the predicted fits based on the model due to Lang et al. Parameters: QS(I)= -2.13 mm/s, η(I) = 0.30, QS(II)= -1.39 mm/s, η(II) = 0.75, energy difference = 74 cm^{-1}, line width = 0.25 mm/s, rate of interconversion = 1.8×10^6 sec^{-1} (50 K), 4.4×10^8 sec^{-1} (250 K), jump angle 90°.

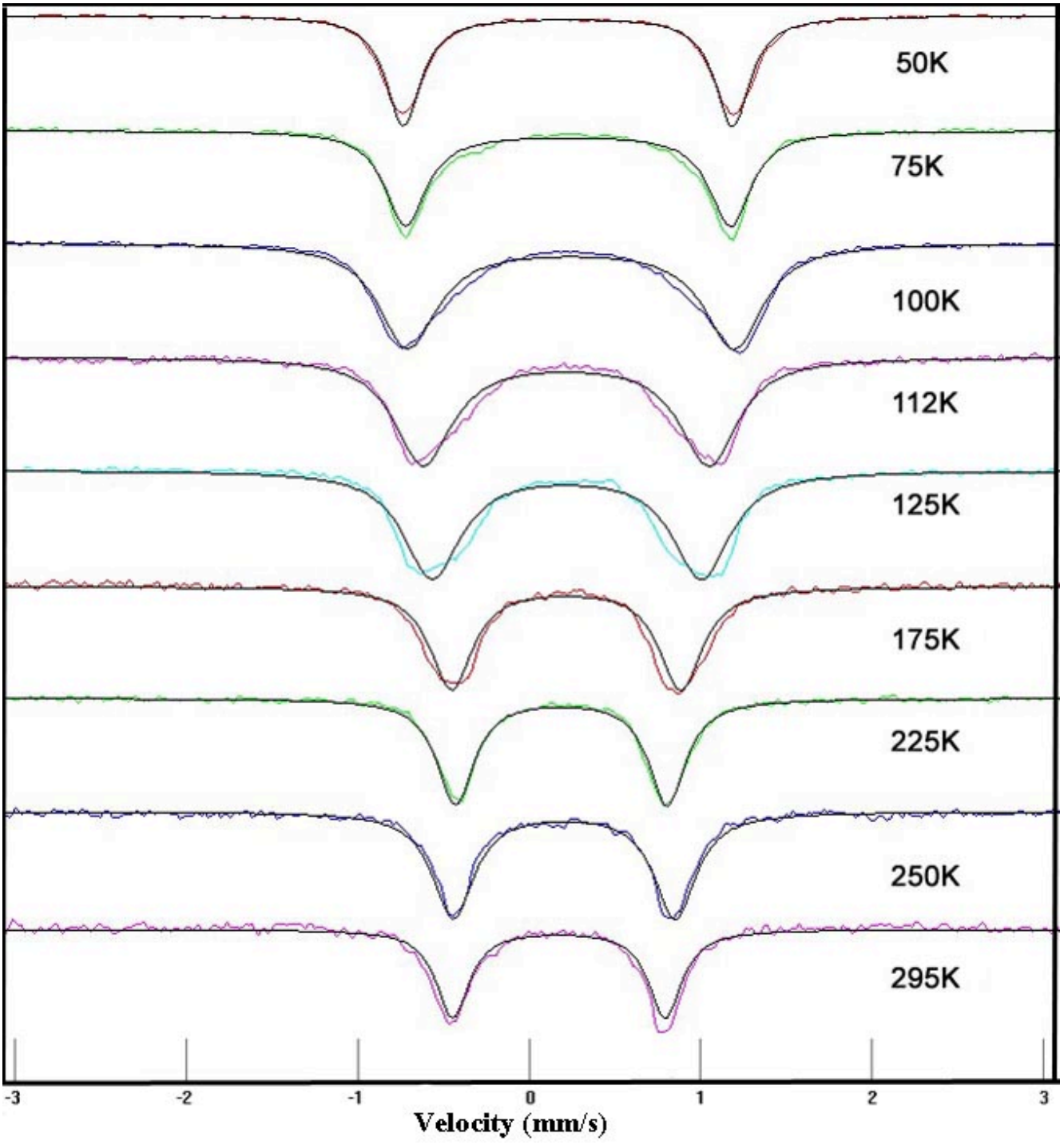

Figure S17. Comparison of the T-dependent experimental data for [Fe(TpivPP)(1-EtIm)(O_2)] (Sample 2)with the predicted fits based on the model due to Oldfield et al. Parameters: QS= -2.09 mm/s, $\eta = 0.12$, energy difference = 123 cm^{-1}, line width = 0.25 mm/s, rate of interconversion = 2.6×10^6 sec^{-1} (50 K), 4.6×10^8 sec^{-1} (250 K), jump angle 90°.

Table S1. Complete Crystallographic Details for [Fe(TpivPP)(1-EtIm)(O_2)]·C_6H_6 and [Fe(TpivPP)(1-MeIm)(O_2)]·0.48C_6H_5Cl ·0.28$C_4H_6N_2$ at 100, 200 and 300K.

chemical formula	$C_{75}H_{78}Fe–N_{10}O_6$	$C_{75}H_{78}Fe–N_{10}O_6$	$C_{75}H_{78}Fe–N_{10}O_6$	$C_{72}H_{74.08}Cl_{0.48}–FeN_{10.56}O_6$	$C_{72}H_{74.08}Cl_{0.48}–FeN_{10.56}O_6$	$C_{72}H_{74.08}Cl_{0.48}–FeN_{10.56}O_6$
FW	1271.32	1271.32	1271.32	1256.23	1256.23	1256.23
a, Å	18.4871(8)	18.5288(9)	18.612(2)	18.537(2)	18.6354(14)	18.7509(16)
b, Å	19.0657(10)	19.2070(10)	19.371(3)	19.176(2)	19.3094(14)	19.4484(17)
c, Å	18.2617(8)	18.4449(8)	18.668(2)	18.280(2)	18.4577(13)	18.6503(16)
α, deg	90	90	90	90	90	90
β, deg	90.010(2)	90.359(2)	90.815(7)	91.074(2)	91.215(2)	91.2670(10)
γ, deg	90	90	90	90	90	90
V, Å^3	6436.7(5)	6564.1(5)	6729.9(16)	6496.7(12)	6640.3(8)	6799.6(10)
space group	$C2/c$	$C2/c$	$C2/c$	$C2/c$	$C2/c$	$C2/c$
Z	4	4	4	4	4	4
temp, K	100(2)	200(2)	300(2)	100(2)	200(2)	300(2)
D_{calcd}, g cm^{-3}	1.312	1.286	1.255	1.280	1.252	1.224
μ, mm^{-1}	0.298	0.292	0.285	0.313	0.307	0.300
final R indices	$R_1 = 0.0704$	$R_1 = 0.0601$	$R_1 = 0.0636$	$R_1 = 0.0714$	$R_1 = 0.0595$	$R_1 = 0.0642$
[I > 2σ(I)]	$wR_2 = 0.1603$	$wR_2 = 0.1492$	$wR_2 = 0.1754$	$wR_2 = 0.1928$	$wR_2 = 0.1691$	$wR_2 = 0.1822$
final R indices	$R_1 = 0.0927$	$R_1 = 0.1255$	$R_1 = 0.1312$	$R_1 = 0.1012$	$R_1 = 0.0775$	$R_1 = 0.0920$
(all data)	$wR_2 = 0.1688$	$wR_2 = 0.1849$	$wR_2 = 0.2205$	$wR_2 = 0.2192$	$wR_2 = 0.1842$	$wR_2 = 0.2070$

Table S2. Complete Crystallographic Details for [Fe(TpivPP)(2-MeHIm)] (crystal A) and Its Oxygenated Derivative.

chemical formula	$C_{70}H_{76}FeN_{10}O_5$	$C_{71}H_{79}FeN_{10}O_{7.5}$	$C_{70}H_{76}FeN_{10}O_{6.3}$
FW	1239.33	1248.29	1214.06
a, Å	18.6056(7)	18.7415(6)	18.8982(19)
b, Å	19.2797(7)	19.4323(6)	19.479(2)
c, Å	17.9414(7)	17.8179(6)	18.313(2)
α, deg	90	90	90
β, deg	90.705(3)	91.609(2)	91.743(4)
γ, deg	90	90	90
V, Å^3	6435.3(4)	6486.6(4)	6738.4(13)
space group	$C2/c$	$C2/c$	$C2/c$
Z	4	4	4
temp, K	100(2)	100(2)	300(2)
D_{calcd}, g cm^{-3}	1.279	1.278	1.197
μ, mm^{-1}	0.296	0.296	0.282
final R indices	$R_1 = 0.0622$	$R_1 = 0.0661$	$R_1 = 0.0873$
[I $> 2\sigma$(I)]	$wR_2 = 0.1754$	$wR_2 = 0.1787$	$wR_2 = 0.2520$
final R indices	$R_1 = 0.0746$	$R_1 = 0.0738$	$R_1 = 0.1019$
(all data)	$wR_2 = 0.1886$	$wR_2 = 0.1848$	$wR_2 = 0.2634$

Table S3. Complete Crystallographic Details for [Fe(TpivPP)(2-MeHIm)] (crystal B) and Its Oxygenated Derivative.

	[Fe(TpivPP)(2-MeHIm)]·2C_2H_5OH	[Fe(TpivPP)(2-MeHIm)(O_2)]·1.8C_2H_5OH	[Fe(TpivPP)(2-MeHIm)(O_2)]·1.8C_2H_5OH	[Fe(TpivPP)(2-MeHIm)(O_2)]·1.8C_2H_5OH	[Fe(TpivPP)(2-MeHIm)(O_2)]·1.6C_2H_5OH	[Fe(TpivPP)(2-MeHIm)0.9(O_2)]·1.4C_2H_5OH
formula	$C_{72}H_{82}FeN_{10}O_6$	$C_{71.6}H_{80.8}FeN_{10}O_{7.8}$	$C_{71.6}H_{80.8}FeN_{10}O_{7.8}$	$C_{71.6}H_{80.8}FeN_{10}O_{7.8}$	$C_{71.20}H_{79.6}FeN_{10}O_{7.6}$	$C_{70.8}H_{79.2}FeN_{10}O_{7.2}$
FW	1239.33	1262.11	1262.11	1262.11	1252.90	1241.29
a, Å	18.6188(9)	18.7058(5)	18.7766(5)	18.7022(6)	18.6840(6)	18.8646(6)
b, Å	19.3919(9)	19.4848(6)	19.5182(6)	19.4689(7)	19.4628(6)	19.5555(7)
c, Å	17.9767(9)	17.8094(5)	18.0082(5)	17.7991(6)	17.7660(5)	18.2826(6)
α, deg	90	90	90	90	90	90
β, deg	90.678(2)	91.598(1)	91.650(1)	91.631(2)	91.612(2)	91.778(2)
γ, deg	90	90	90	90	90	90
V, Å^3	6490.1(5)	6488.6(3)	6597.0(3)	6478.2(4)	6457.9(3)	6741.3(4)
space group	$C2/c$	$C2/c$	$C2/c$	$C2/c$	$C2/c$	$C2/c$
Z	4	4	4	4	4	4
temp, K	100(2)	100(2)	200(2)	100(2)	80(2)	300(2)
D_{calcd}, g cm^{-3}	1.268	1.297	1.271	1.294	1.289	1.223
μ, mm^{-1}	0.293	0.292	0.292	0.297	0.297	0.284
final R indices	$R_1 = 0.0618$	$R_1 = 0.0760$	$R_1 = 0.0469$	$R_1 = 0.0731$	$R_1 = 0.0784$	$R_1 = 0.0707$
[I $> 2\sigma$(I)]	$wR_2 = 0.1779$	$wR_2 = 0.1828$	$wR_2 = 0.1347$	$wR_2 = 0.1791$	$wR_2 = 0.1835$	$wR_2 = 0.2030$
final R indices	$R_1 = 0.0723$	$R_1 = 0.0813$	$R_1 = 0.0543$	$R_1 = 0.0774$	$R_1 = 0.0818$	$R_1 = 0.0852$
(all data)	$wR_2 = 0.1901$	$wR_2 = 0.1854$	$wR_2 = 0.1425$	$wR_2 = 0.1813$	$wR_2 = 0.1851$	$wR_2 = 0.2144$